ELSEVIER

Cement & Concrete Composites 26 (2004) 463–471

Cement & Concrete Composites

www.elsevier.com/locate/cemconcomp

Concrete pavement temperature prediction and case studies with the FHWA HIPERPAV models

A.K. Schindler [a,*], J.M. Ruiz [b], R.O. Rasmussen [b], G.K. Chang [b], L.G. Wathne [c]

[a] Auburn University, 221 Harbert Engineering Center, Auburn, AL 36849, USA
[b] The Transtec Group, Inc., 1012 East 38 1/2 Street, Austin, TX 78751, USA
[c] FHWA/SaLUT Inc., 400 7th Street, SW, Room 3118, Washington, DC 20590, USA

Abstract

High performance concrete paving (HIPERPAV) is a concrete paving software product sponsored by the Federal Highway Administration. The objective of this paper is to present recent improvements made to the temperature prediction model, and to illustrate that this model can be used to predict the in-place temperature development in portland cement and fast-setting hydraulic cement concrete paving applications. The concrete temperature prediction model consists of a transient one-dimensional finite-difference model, which includes the heat of hydration of the cementitious materials and the heat transfer mechanisms of thermal conduction, convection (including evaporative cooling), solar radiation, and irradiation. A new model is introduced to account for the effect of evaporative cooling, which may occur on the concrete surface. To validate the temperature model, the concrete temperatures measured in the field were compared to the concrete temperatures predicted with the temperature model. The HIPERPAV temperature model produced accurate predictions of the in-place temperature development of hydrating concrete.

Keywords: Temperature prediction; Hydration models; Heat transfer; Fast-setting hydraulic cement; Adiabatic calorimeter test; Evaporative cooling; Concrete pavements; HIPERPAV

1. Introduction

High performance concrete paving (HIPERPAV) is a concrete paving software product sponsored by the Federal Highway Administration (FHWA) [1]. HIPERPAV enables users to evaluate the complex interactions that affect the concrete pavement behavior at early ages. Adequate selection and control of these factors (mixture proportions, curing conditions, time of saw cutting, time of placement, etc.) will increase the chances of good performance throughout the intended design life of the pavement. Using HIPERPAV questions pertaining to material selection, pavement design, and construction operations can be evaluated, as its integrated approach captures most aspects of concrete pavement construction and provides a systems approach to analyze the first 72 h after construction.

The temperature prediction model in HIPERPAV is paramount to its success. The predicted concrete temperatures drive a number of key behavior models in HIPERPAV including strength and stiffness gain (based on the Arrhenius maturity concept), creep, and thermal expansion properties [1]. Prediction of the in-place pavement temperatures, as affected by the environment and cement hydration, has a number of applications during early ages and in the long term. These applications include the following:

- *Early-age and long-term pavement behavior*: Fluctuations in temperature produce expansion and contraction movements in concrete pavements, which lead to the development of stresses and possibly cracking, which may significantly affect the pavement's early-age and long-term performance [1].
- *Strength prediction*: Through the maturity method [2] the strength development of in-place concrete can be predicted. Once the in-place strength is predicted it can be used among other applications to evaluate causes for distress, earliest sawcutting time, opening to traffic time, and risk of crack formation.
- *Risk of plastic shrinkage cracking*: Prediction of evaporation rate is a function of concrete temperature,

* Corresponding author: Tel.: +1-334-844-6263; fax: +1-334-844-6290.
E-mail address: antons@eng.auburn.edu (A.K. Schindler).

0958-9465/$ - see front matter © 2003 Elsevier Ltd. All rights reserved.
doi:10.1016/S0958-9465(03)00075-1

wind speed, air temperature, and relative humidity [3]. With the temperature model, evaporation rate can be determined and mitigation measures to prevent plastic shrinkage cracking can be evaluated prior to the occurrence of undesirable conditions.

- *Temperature gradients*: The thermal gradients at final set can be determined with the temperature model presented in this paper. It has been reported that the initial thermal gradient at setting (built-in curling) plays a major role in the long-term performance of jointed concrete pavements [4].

1.1. Paper objectives

The objective of this paper is to present the temperature prediction model, and its application to two very different real world projects. The application of the temperature model will be evaluated for portland cement concrete (PCC) and fast-setting hydraulic cement concrete (FSHCC) paving applications. As some of the models have been documented in previous publications [1,5,6], only improvements to the original models will be presented in detail here.

2. Concrete temperature prediction

During the hydration of concrete under field conditions, the concrete temperature development is determined by the balance between heat generation from the cementitious materials and heat exchange with the structure and its surroundings. The surroundings could either be an additional source of heat or at a lower temperature than the hydrating concrete. Fig. 1 shows a simplification of the process used to predict concrete temperatures under field conditions, which is categorized into the following three components:

- *Concrete heat of hydration*: Numerous factors influence the concrete heat of hydration and the interaction of these factors are very complex. The cement composition, cement fineness, amount of cement, presence of mineral and chemical admixtures, and the temperature of hydration primarily influence the heat of hydration. All of the factors and their interactions are considered in the systems approach adopted in HIPERPAV. More details will be provided on this phase in Section 2.1.
- *Environmental effects*: As is the case with most chemical reactions, the hydration of cement is strongly affected by its current temperature and moisture state. Environmental conditions fluctuate through diurnal cycles, and parameters such as ambient air temperature, wind speed, relative humidity, solar radiation, and cloud cover have constantly changing values. This causes the hydration behavior under field conditions to be very different from hydration under laboratory conditions. Conditions imposed during laboratory tests are often adiabatic or isothermal, which do not reflect the in-place hydration environment. This necessitates that the environmental effects encountered during construction and curing be accounted for when the in-place properties of concrete structures are predicted. In HIPERPAV, environmental data for any location in the United States is generated based on averaged 30-year historical data obtained from a weighted-average of nearby weather stations.
- *Heat exchange*: In concrete placed under field conditions, heat will be transferred to and from the surroundings. Heat transfer mechanics have to be considered to model the transient heat exchange. As shown in Fig. 1, the effects of various parameters including base temperature, curing methods, type of support materials, aggregate type used, slab thickness, and concrete surface color are all accounted for with the heat transfer model included in HIPERPAV. Some details of the heat transfer models have been previously published [1,5]. However, details of additional model improvements are provided in Section 2.2.

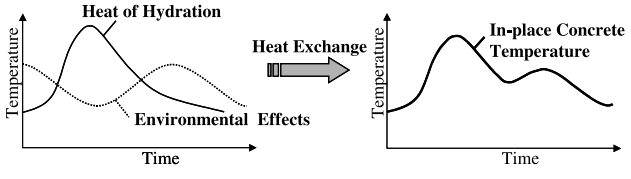

FACTORS CONSIDERED

Heat of Hydration	Environmental Effects	Heat Exchange
Cement Composition	Air Temperature	Base Temperature
Cement Fineness	Wind Speed	Curing method
Amount of cement	Relative Humidity	Support material
w/cm ratio	Solar Radiation	Aggregate type
Admixtures	Atmospheric Pressure	Slab Thickness
Mix Temperature	Cloud Cover	Surface color

Fig. 1. Overview of primary model components and the variables considered.

2.1. Cement hydration modeling

The hydration reaction of cement is an exothermic process, in which heat is liberated during the reaction of the cementitious materials with water. The heat of hydration is the amount of heat that is released into the system due to the hydration processes of the cementitious materials. There are a number of factors that affect the hydration of the cement, and it is a complex problem to incorporate all these factors into a mechanistic hydration model in such a way that the temperature development can accurately be predicted.

This problem is overcome by submitting the concrete to an adiabatic calorimeter test, where there is no in-

terchange of heat with the surroundings [7]. From the test results, the rate of heat evolution with progressive hydration for a specific concrete mixture can be determined. HIPERPAV uses various hydration curves for different cement types and combinations of admixtures, obtained from adiabatic calorimeter tests, to characterize the temperature generation of a concrete mixture [5].

During the initial development of HIPERPAV, the scope of the concrete paving materials was limited to PCC. This type of cement typically only has one main hydration peak, therefore, its behavior can accurately be modeled with a one-peak hydration model [1,5]. However, when high-alumina cements are used, the presence of two main hydration peaks is not uncommon. Sulfoaluminate cements rely on the development of ettringite in the hardened cement paste, which occurs very early and is the cause of the first hydration peak. For instance, during this project adiabatic calorimeter tests were performed on a FSHCC and two distinct main peaks were noticed. In Section 3.2 the results of the adiabatic calorimeter tests are presented and discussed.

Since the heat of hydration model used in HIPERPAV was not initially tailored to consider cements with two hydration peaks, some modification of the model was necessary. The best-fit model to incorporate the effect of these two peaks was developed for use during the temperature prediction. The heat of hydration (Q_h) released into the system due to the hydration processes of the cementitious materials is mathematically defined as follows:

$$Q_h = H_{u1} C \psi_1 \frac{\kappa_1}{t_1} \cdot \frac{[\ln(\tau_1)]^{-(1+\kappa_1)}}{\tau_1} \cdot e^{\left[-\frac{\phi}{R}\left(\frac{1}{T+273}-\frac{1}{T_r+273}\right)\right]} + H_{u2} C \psi_2 \frac{\kappa_2}{t_2} \cdot \frac{[\ln(\tau_2)]^{-(1+\kappa_2)}}{\tau_2} \cdot e^{\left[-\frac{\phi}{R}\left(\frac{1}{T+273}-\frac{1}{T_r+273}\right)\right]}, \quad (1)$$

where Q_h = generated heat of hydration (W/m^3), H_{u1} = total heat of hydration for first hydration peak (J/kg), H_{u2} = total heat of hydration for second hydration peak (J/kg), C = cementitious materials content (kg/m^3), κ_1, κ_2 = adiabatic hydration shape parameters for first and second hydration peaks, t_1, t_2 = adiabatic hydration time parameters for first and second hydration peaks (s), τ_1 = age parameter for first hydration peak, defined as: $1 + t_e/t_1$, τ_2 = age parameter for second hydration peak, defined as: $1 + t_e/t_2$, ψ_1 = degree of hydration for first hydration peak, defined as: $e^{-(\ln \tau_1)^{-\kappa_1}}$, ψ_2 = degree of hydration for second hydration peak, defined as: $e^{-(\ln \tau_2)^{-\kappa_2}}$, t_e = equivalent age (s) at concrete chronological age t, defined as:

$$\sum_{t=0}^{\text{age}} \left[e^{\left[-\frac{\phi}{R}\left(\frac{1}{T+273}-\frac{1}{T_r+273}\right)\right]} \cdot \Delta t \right] \quad (2)$$

Δt = the chronological time interval (s), Φ = activation energy (J/mol), R = universal gas constant (8.3144 J/mol/°C), T = average nodal temperature during Δt, (°C), and T_r reference temperature, 20 °C.

The formulation of the heat of hydration in Eq. (1) is similar to the one peak hydration model previously used in HIPERPAV and the reader is referred to McCullough and Rasmussen [1] if more information regarding the formulation is required. The total heat of hydration (H_{u1},H_{u2}) varies greatly with the cement composition, and the type of mineral admixtures used. The quantities of C_3A and C_3S are primarily responsible for heat evolution at early ages. Each cement constituent has been found to have a unique heat of hydration, and the total heat of hydration can be estimated directly from the cement chemistry by multiplying the percentage of the total mass of each constituent by its individual heat of hydration contribution [1,8]. The total heat of hydration can also be determined from adiabatic calorimeter test results.

The degree of hydration (ψ) is a measure of the quantity of the hydration products formed and is a function of the equivalent age, with ψ varying between 0% at the start of hydration, and 100% when hydration is completed. Experimentally the degree of hydration can be calculated from the adiabatic calorimeter test results. It has been shown that the heat released at a given time divided by the total heat available provides a good measure of the degree of hydration [9].

2.2. Heat transfer models

The temperature development in the concrete structure is determined by the balance between heat generation in the concrete and heat exchange with the environment. Over the course of its development, HIPERPAV has employed two different temperature prediction models. Originally, the temperature prediction model was a transient two-dimensional finite-element model. However, this procedure had proven to require excessive solution times. The model has since been replaced by a one-dimensional finite-difference approach, which allows quicker execution without a compromise in accuracy. A two-dimensional heat transfer model is in general not necessary in pavement applications in which it is assumed that horizontal surfaces are large compared to the vertical slab thickness and that temperature varies only in the vertical direction.

The boundary conditions for the heat transfer analysis include the following heat transfer mechanisms: conduction, convection (including evaporative cooling), irradiation, and solar absorption at the top surface of the pavement. The HIPERPAV models for each of these effects have been presented in detail in the past [1,5]. However, since that time, improvements have been made to the convection model to include the effects of evaporative cooling when surface water and free water from the hydrated cement paste evaporates. In the

following section, the evaporative cooling model will be introduced, and in Section 3 the model will be validated.

2.2.1. Heat transfer due to evaporative cooling

When evaporation of the water from a surface occurs, the energy associated with the phase change is the latent heat of vaporization, which causes evaporative cooling. The amount of energy dissipated through evaporative cooling can be determined as follows [10]:

$$q_{\text{evap}} = -E_{\text{c}} \cdot h_{\text{lat}}, \tag{3}$$

where q_{evap} = heat flux due to evaporative cooling (W/m^2), E_{c} = evaporation rate of water from concrete surface (kg/m^2/s), and h_{lat} = latent heat of vaporization (J/kg).

The latent heat of vaporization is the quantity of heat, required to evaporate 1 g of water. The latent heat of vaporization is a function of the surface water temperature, and can be approximated as follows [10]:

$$h_{\text{lat}} = 2,500,000 + 1859 \cdot T_{\text{sw}}, \tag{4}$$

where T_{sw} = temperature of the surface water (°C).

The evaporation rate of water from free surfaces (E_{w}) is driven by the difference in vapor pressure between the air and the evaporating water. Menzel was the first to publish a graphical solution to predict evaporation from lakes and other bodies of water [11]. ACI Committee 305 recommends a version of Menzel's nomograph to calculate evaporation rate of water from free surfaces as indicator to evaluate the risk of plastic shrinkage cracking [3]. However, the rate of water evaporation from a concrete surface (E_{c}) is equal to the evaporation rate of water from free surfaces (E_{w}) only when the concrete surface is covered with bleed water [12]. It has been shown that the amount of water that evaporates from the concrete surface is dependent on the bleeding rate, the concrete surface texture, and the curing method used [12,13]. The bleeding rate for a specific mixture is a complex issue that is currently not well understood, and it has been shown to be influenced by the water/cement ratio, cement content, concrete degree of hardening, and type of cementitious materials used [12,14].

After laboratory tests, Al-Fadhala and Hover [12] presented the following useful formulation to determine the rate of water loss from a concrete surface as compared to the water loss from a free water surface:

$$E_{\text{c}}/E_{\text{w}} = \exp[-(t/a)^{1.5}], \tag{5}$$

where E_{c} = evaporation rate from a concrete surface (kg/m^2/h), E_{w} = evaporation rate from a free water surface (kg/m^2/h), t = concrete age (h), and a = time constant (3.75 h for concrete and 6.16 h for mortar).

Eq. (5) was developed from test data obtained from concrete specimens 60-mm deep, and Type I cement was used. The formulation does not account for the effect of surface texture or different curing methods. It was recommended that the time parameter, a, be determined for a given mixture [12]. Evaporative cooling may occur even at low evaporation rates. It has been noted that plastic shrinkage cracks occurred at evaporation rates ranging from 0.2 to 0.7 kg/m^2/h, as opposed to the threshold value of 1 kg/m^2/h suggested by ACI Committee 305 [14].

Due to the limited information available on the subject, the formulation above was implemented in the HIPERPAV temperature prediction algorithms. The accuracy of the model is evaluated in Section 3, which covers the field validation of the temperature model.

3. Validation of the temperature prediction models

In order to assess the accuracy of the HIPERPAV temperature model for PCC and FSHCC paving applications, data was evaluated from two case studies. This section will briefly present the data collected from each case study, and the validation process will be presented and discussed.

3.1. Validation plan

Two construction sites were selected, one located in the State of North Carolina and the other in the State of California. The on-site monitoring plan consisted of recording the pavement layer structure, concrete mixture proportions, construction operations, pavement temperatures, and the environmental conditions that prevailed during construction and curing of the newly placed concrete. Environmental conditions were monitored by an on-site weather station and included the air temperature, wind speed, solar radiation, and relative humidity. For the California site, solar radiation values were obtained from a nearby weather station. Raw materials were also collected from the site to perform additional laboratory tests such as adiabatic calorimetry. The slab temperatures were measured by thermocouples located at three locations: 25 mm from the top surface, mid-depth, and 25 mm from the bottom surface. The mid-depth thermocouple for the North Carolina site instrumentation produced erroneous results and was not used in subsequent analysis. Table 1 provides a summary of the variables collected for each case study, and the following sections will provide more information about each of the case studies.

3.1.1. North Carolina field site

This seven mile reconstruction project was located on Interstate Highway 77 in Surry County, North Carolina, and construction occurred in May 1999. The pavement consisted of a 280-mm thick doweled jointed plain concrete pavement on top of an existing concrete pavement separated by a leveling bond breaking hot mix

Table 1
Summary of variables for both case studies

Parameter	North Carolina Site	California Site
Pavement design and materials		
Pavement thickness (mm)	280	230
Subbase type	HMA	Cement treated
Subbase thickness (mm)	50	150
Concrete mixture design		
Cement	ASTM C150 Type I/II	Calcium sulfoaluminate[a]
Coarse aggregate type	Phyllite	River Gravel
Cement content (kg/m^3)	250	390
Mineral admixtures	Class F Fly ash 75 kg/m^3	–
Water content (kg/m^3)	141	179
Coarse aggregate content (kg/m^3)	1147	1115
Fine aggregate content (kg/m^3)	834	676
Water reducer (ml/m^3)	1060	Unknown
Air entrainment agent (ml/m^3)	106	Unknown
Environmental conditions		
Maximum air temperature (°C)	27	31
Minimum air temperature (°C)	9	14
Relative humidity range (%)	36–97	36–44
Wind speed range (km/h)	0–3.6	0–3.4
Maximum solar radiation (W/m^2)	1249	1158
Cloud cover conditions	40% cloudy day 1, Sunny on day 2 and 3	Sunny on all days
Construction operations		
Construction day and time	05/22/99 12:30 pm	07/24/99 4:42 am
Fresh concrete temperature (°C)	27	31
Initial subbase temperature (°C)	26	23
Curing method	White curing compound	White curing compound
Time of curing application	05/22/99 1:50 pm	07/24/99 5:06 am
Material properties		
Hydration parameters, 1st peak[b]	$t_1 = 16.931$ h, $\kappa_1 = 1.188$	$t_1 = 1.312$ h, $\kappa_1 = 0.768$
Hydration parameters, 2nd peak[b]	–	$t_2 = 8.559$ h, $\kappa_2 = 4.093$
Total heat of hydration (J/g)	$H_{u1} = 483$, $H_{u2} = 0$	$H_{u1} = 272.6$, $H_{u2} = 48.3$
Activation energy[c] (J/mol)	42,000	45,000
Soil specific heat[c] (J/(kg °C)	1050	1005
Thermal conductivity of hardened pavement concrete[c] (W/m/°C)	2.7	3.6
Soil thermal conductivity[c] W/m/°C	1.4	3.3

[a] Fast-setting hydraulic cement, specified to have a 5-h flexural strength of 2.1 MPa.
[b] Hydration parameters were determined by adiabatic calorimeter tests.
[c] Values were not experimentally obtained. Values based on published data [1,5].

asphalt (HMA) base. The cementitious materials consisted of ASTM C 150 Type I/II cement replaced by mass with 23% Class F fly ash. A total cementitious materials content of 6 sacks per cubic yard was used.

3.1.2. California field site

This project was located on Interstate 10 in Pomona, California, and construction occurred in July 1999. The project incorporated the rehabilitation of an old jointed concrete pavement by replacing the deteriorated slabs and retrofitting dowel bars to the slabs in good condition. A FSHCC mix containing calcium sulfo-aluminate was used to provide high concrete strengths at early ages to allow opening to traffic in a short period of time. The FSHCC was specified to have a 5-h flexural strength of 2.1 MPa.

The pavement consisted of a 230-mm thick doweled jointed plain concrete pavement on top of a 100–150-mm thick cement treated base (CTB). A 100–150-mm thick aggregate base supported the CTB. A plastic sheet was also used as bond breaker between the newly placed concrete and the existing CTB. During the day of instrumentation, approximately 60 of the existing 15 feet slabs were removed and replaced.

3.2. Concrete hydration characterization

The results from the adiabatic calorimeter tests for both case studies are shown in Fig. 2. (Note: The concrete age in Fig. 2 is in terms of chronological age and this convention will be used for the remaining figures in this paper.) In Fig. 2(a) the adiabatic test results show

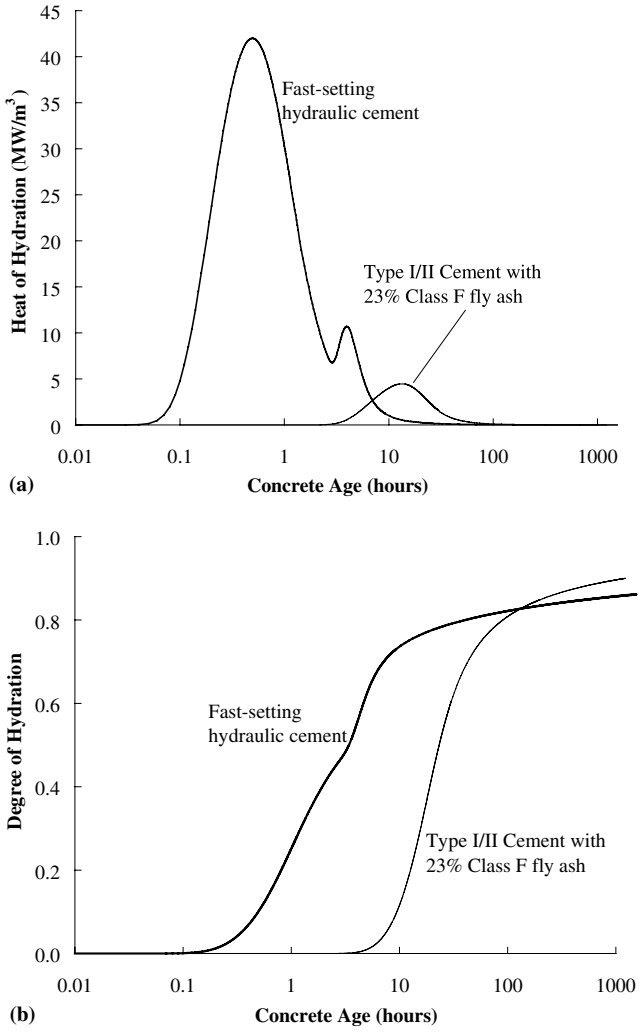

Fig. 2. (a) Heat of hydration for FSHCC and Type I/II cement with fly ash, (b) degree of hydration for FSHCC and Type I/II cement with fly ash.

that there are two distinct heat of hydration peaks that occur during the hydration process of the FSHCC. The start of the first heat of hydration peak of the FSHCC occurs within 1 h after water is added, whereas the peak for the Type I/II cement with fly ash occurs after 14 h of hydration. The second peak for the FSHCC occurs around 4 h after water is added to the mixture. The presence of two heat of hydration peaks in the FSHCC is a characteristic of cement with significant quantities of alumina.

The degree of hydration for both case studies are shown in Fig. 2(b) and it may be seen that the hydration progress of the FSHCC occurs at a significantly faster rate than the Type I/II cement with fly ash. This graph clearly shows the effect of using the FSHCC for fast-track construction as it reaches a degree of hydration of 70% within 7 h, whereas the mixture with Type I/II cement with fly ash is only at 5% after the same time has elapsed. The hydration parameters for both mixtures used in the case studies are listed in Table 1.

3.3. Evaporative cooling effects

The presence and effect of evaporative cooling may be identified from the temperature history of the thermocouples located close to the top of the pavement surface, as shown in Figs. 3(a) and 4(a). In Fig. 3(a), an apparent reduction in concrete temperatures may be identified. For concrete that was placed a little after noon, a temperature increase was expected due to the presence of solar radiation, high air temperatures, and heat of hydration. However, there was only a slight increase (5 °C) in the surface concrete temperature during the first 12 h. The temperature increase after 24 h is in excess of 18 °C when the effect of solar radiation and convection occurred without the effect of evaporative cooling. It may be concluded that evaporative cooling occurred during early-ages and prevented a marked increase in concrete temperatures due to hydration, solar radiation, and convection.

In Fig. 4(a), the surface temperature initially increases rapidly due to the heat of hydration of the FSHCC, but then after about 2 h there was an unexpected sudden decrease in concrete temperature. The section was paved at around 5 am, and the decrease in concrete temperatures started to occur at around 7 am, i.e. as soon as the solar radiation from the rising sun started to reach the freshly placed concrete. The effect of evaporative cooling is very pronounced as the drop in temperatures between 2 and 5 h after placement also progressed into the mid-depth and bottom of the slab. Without the effects of evaporative cooling, the concrete temperatures are expected to rise after sunrise as the heat of hydration and heat gain from solar effects are superimposed into the system. The evaporation rate from a free water surface was calculated for this case study with Menzel's equation [11]. Due to the low relative humidity and high concrete temperatures, the evaporation rate exceeded a value of 0.5 kg/m^2/h for most of the early-age periods and it was as high as 3.6 kg/m^2/h 13 h after placement. From this case study, it may also be concluded that the effects of evaporative cooling was also present at early ages.

During the prediction of concrete temperatures, the effects of evaporative cooling were modeled to account for the phenomenon that may clearly be identified after a review of the temperature histories. The evaporative cooling model presented in Section 2.2.1 was used. The best-fit time parameter, a, was determined to account for the very early-age evaporative cooling heat losses that occurred at each field site. Time parameters of 6.0 and 8.0 were used, for the PCC and FSHCC respectively. The effect of these time parameters on the E_c/E_w ratio is shown in Fig. 5. Note that larger time para-

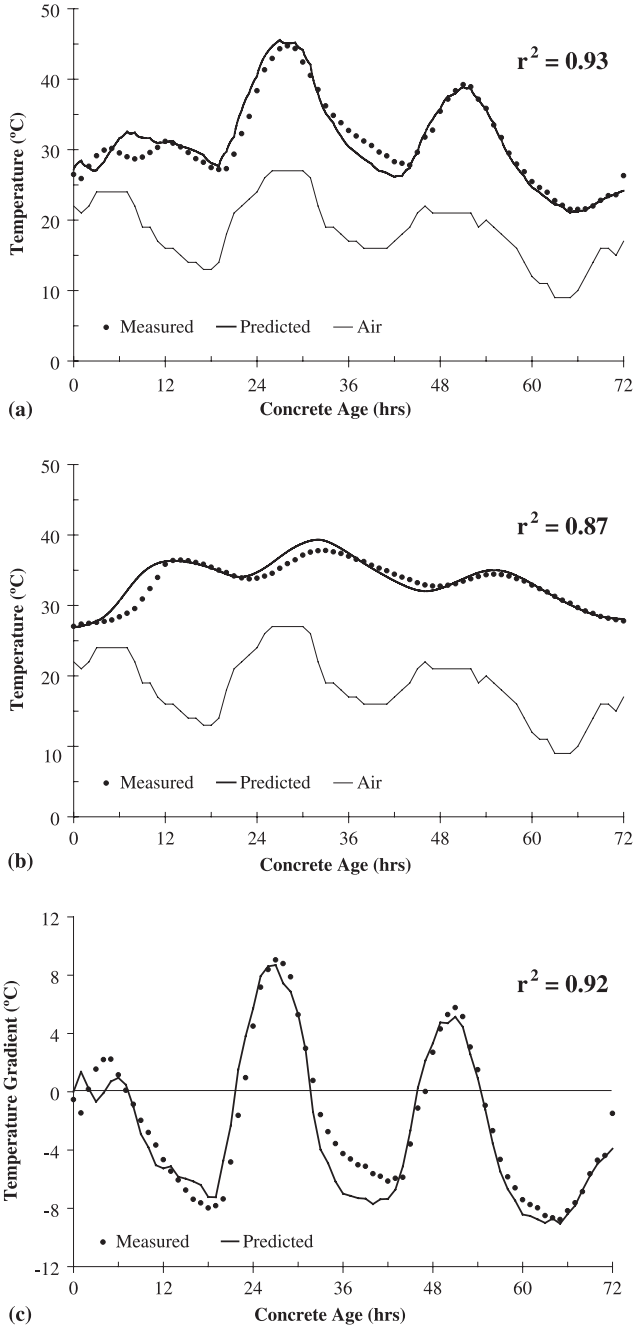

Fig. 3. (a) Temperatures, 25 mm from the top surface for the North Carolina site, (b) temperature, 25 mm from the bottom surface for the North Carolina site, (c) linear temperature gradients for the North Carolina site.

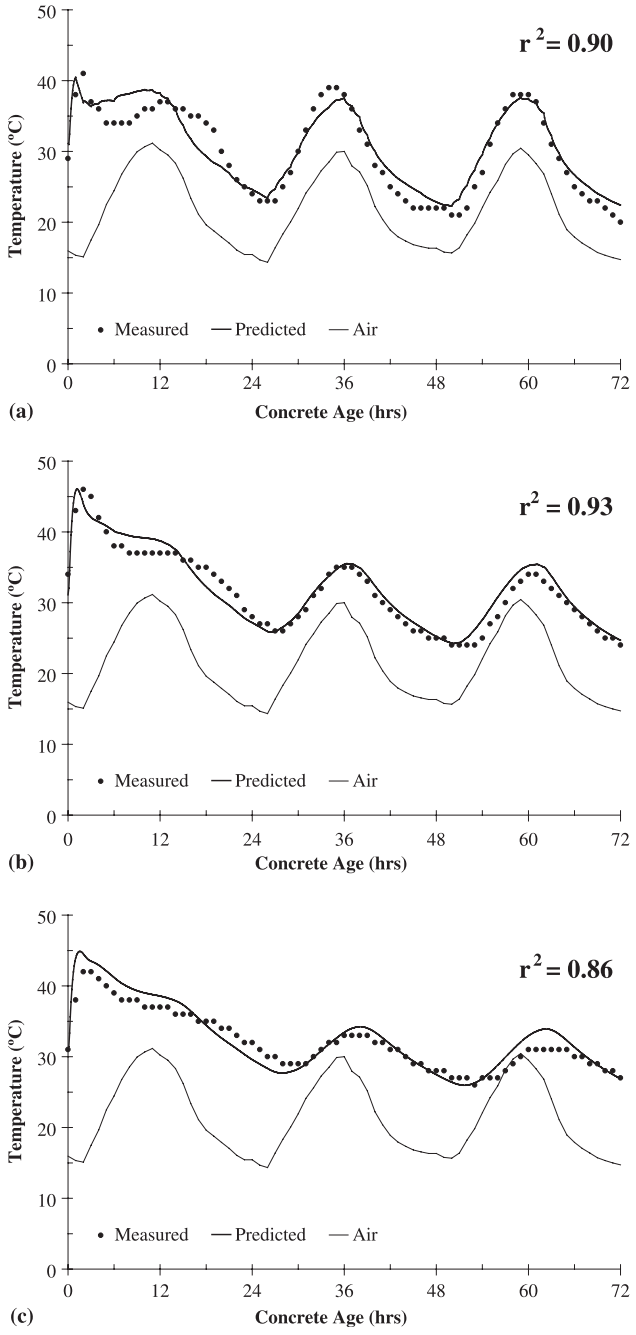

Fig. 4. (a) Temperatures, 25 mm from the top surface for the California site, (b) temperatures at mid-depth for the California site, (c) temperatures, 25 mm from the bottom surface for the California site.

meters produce longer periods and higher magnitudes of possible evaporative cooling. It is unknown why the FSHCC pavement required a larger time parameter as compared to the PCC pavement. The time parameter used for the North Carolina (PCC) case study was similar to the mortar value recommended by Al-Fadhala and Hover [12]. The apparent increase in evaporation could be attributed to the thicker pavement section (280 mm) as compared to the 60-mm thick laboratory specimens. Thicker sections would develop higher hydrostatic pressures, which might cause increased bleeding and water loss.

3.4. Pavement temperature prediction

To validate the temperature model, the concrete temperatures measured in the field were compared to the simulated concrete temperatures predicted with the

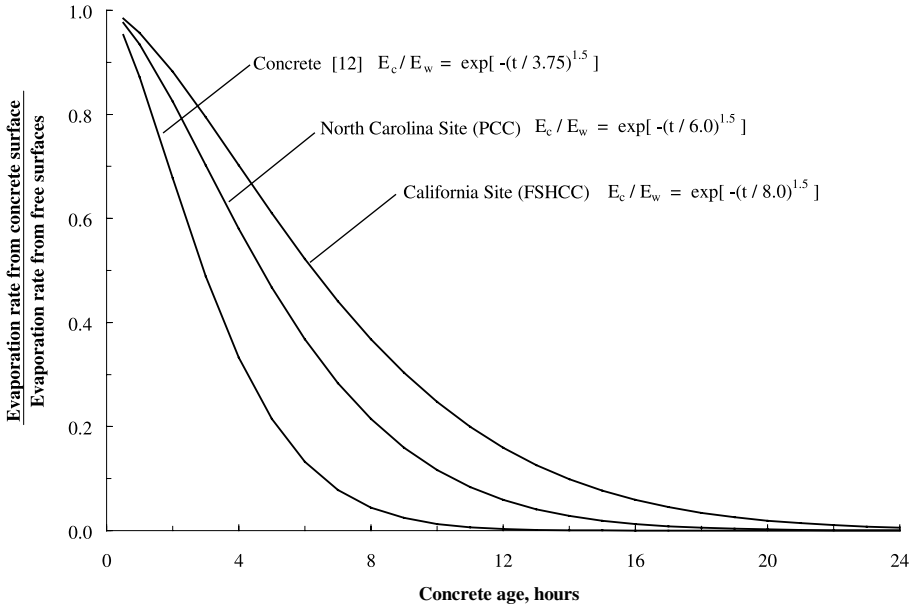

Fig. 5. E_c/E_w development with time for the field sites.

temperature model. The measured versus predicted temperatures throughout the depth of the slab were compared, as well as the temperature gradient from top to bottom of the slab. The results of the temperature prediction are presented in Figs. 3 and 4.

To assess the fit of the theory to the experimental values, a least square regression fit was performed and the coefficient of determination (r^2-value) calculated. Comparison of the measured versus predicted pavement temperature was used in the evaluation of prediction accuracy, as the r^2-value with this procedure takes into account possible systematic trends in over-prediction or under-prediction. The coefficient of determination with this procedure is determined with only two variables, which allows the use of the simple linear regression model, which guarantees appropriate use of the r^2-value.

The r^2-values obtained for each temperature prediction is shown on temperature plots in Figs. 3 and 4. The average r^2-values were 0.91 and 0.88 for the PCC and FSHCC case studies respectively. From all the r^2-values obtained during this analysis, the lowest individual r^2-value was 0.81 for temperature gradient in the California (FSHCC) case study. From the high r^2-values and the prediction trends shown in Figs. 3 and 4, it may be concluded that HIPERPAV with the modified hydration and evaporative cooling model is able to provide an accurate estimate of the temperatures of hydrating PCC and FSHCC paving applications.

4. Summary and conclusions

This paper demonstrates the capabilities of HIPERPAV's temperature prediction model over two different concrete mixtures: conventional versus fast-setting. The early-age temperature development of concrete can be estimated from knowledge of cement composition, cement content, admixtures, thermal characteristics of the concrete, slab thickness, and the environmental conditions that occur during paving and curing. Major findings from this paper are as follows:

- Adiabatic calorimeter tests provide a means of characterizing concrete hydration with time. Using results from adiabatic calorimeter tests, HIPERPAV can account for the effects that different mixture proportions and constituents have on the heat of hydration of concrete.
- Fast-setting hydraulic cement containing calcium sulfoaluminate exhibits two main heat development peaks during hydration. A model is presented to incorporate the effect of these two hydration peaks into HIPERPAV's temperature prediction routine.
- Heat transfer due to evaporative cooling may significantly reduce temperatures in hydrating concrete. Concrete temperatures measured in the field indicated that evaporative cooling occurred during early ages and prevented a marked increase in concrete temperatures due to hydration, solar radiation, and convection. A model is presented that accounts for the effect of evaporative cooling.
- The HIPERPAV temperature model is able to produce good predictions of the temperatures measured in the field. The average r^2-values were 0.91 and 0.88 for the PCC and FSHCC case studies respectively. From the prediction trends presented in this paper, it may be concluded that HIPERPAV with the modified hydration and evaporative cooling

model is able to provide an accurate estimate of the temperatures of hydrating PCC and FSHCC paving applications.

Acknowledgements

The authors would like to extend their appreciation and gratitude to the sponsor of the HIPERPAV system, the Federal Highway Administration. The authors would especially like to thank, among others, Dr. Stephen Forster, Mr. Suneel Vanikar, Mr. Mike Dallaire, Mr. Mark Swanlund, Mr. Gary Crawford, and Mr. Fred Faridazar. The authors are also grateful for the guidance and inspiration of Dr. B. Frank McCullough from the University of Texas at Austin.

References

[1] McCullough BF, Rasmussen RO. Fast track paving: concrete temperature control and traffic opening criteria for bonded concrete overlays. Task G, Final Report, FHWA, US Department of Transportation; 1998.

[2] Carino NJ. Chapter 5: The maturity method. In: Malhotra VM, Carino NJ, editors. CRC Handbook on nondestructive testing of concrete. Florida: CRC Press; 1991.

[3] ACI 305. Hot weather concreting—ACI 305R-99. Farmington Hills, Michigan: American Concrete Institute; 1999.

[4] Yu HT, Khazanovich L, Darter MI, Ardani A. Analysis of concrete pavement responses to temperature and wheel loads measured from instrumented slabs. Transportation Research Record No. 1639; 1998. p. 94–101.

[5] Ruiz JM, Schindler AK, Rasmussen RO, Kim PJ, Chang GK. Concrete temperature modeling and strength prediction using maturity concepts in the FHWA HIPERPAV software. Proceedings of the seventh international conference on concrete pavements, September 2001, Orlando, Florida. p. 9–13.

[6] Ruiz JM, Kim PJ, Schindler AK, Rasmussen RO. Validation of HIPERPAV for prediction of early age jointed concrete pavement behavior. Transportation Research Record 1778, 2001, Washington, DC. p. 17–25.

[7] Morabito P. Methods to determine the heat of hydration of concrete. In: Springenschmid R, editor. Prevention of thermal cracking in concrete at early ages. London: E&FN Spon; 1998. p. 1–25.

[8] Mindess S, Young TF. Concrete. New Jersey: Prentice-Hall Inc; 1981.

[9] Van Breugel K. Simulation of hydration and formation of structure in hardening cement based materials. 2nd ed. Netherlands: Delft University Press; 1997.

[10] ASHRAE. 1993 ASHRAE Handbook. I-P Ed., American Society of Heating, Refrigerating and Air-Conditioning Engineers, Atlanta; 1993.

[11] Menzel CA. Causes and prevention of crack development in plastic concrete. Proceedings of the Portland Cement Association; 1954. p. 130–36.

[12] Al-Fadhala M, Hover KC. Rapid evaporation from freshly cast concrete and the Gulf environment. Construct Build Mater 2001;15:1–7.

[13] Rochefort JL, McCullough BF, Dossey T, Fowler DW. Evaluation of the effects of the tining operation on the performance of portland cement concrete pavements. Research Report 4978-1, The Center for Transportation Research, October 2000, Austin, TX.

[14] Almusallam AA, Maslehuddin M, Abdul-Waris M, Khan MM. Effect of mix proportions on plastic shrinkage cracking of concrete in hot environments. Construct Build Mater 1998;12:353–8.